Progress In Electromagnetics Research C, Vol. 119, 161–175, 2022

Design and Characteristics Mode Analysis of a Cantor Set Fractal Monopole Antenna for IoT Applications

Geeta Kalkhambkar[1, *], Rajashri Khanai[2], and Pradeep Chindhi[3]

Abstract—A four-level iterated cantor set fractal antenna for Internet of Things (IoT) applications is proposed in this work. The proposed antenna operates at 2.4 GHz and for the range of 5 GHz to 8.5 GHz. In the 5 GHz to 8.5 GHz range it covers a Wi-Fi802.11 Standard (4.9 GHz, 5 GHz, 5.9 GHz, 6 GHz), 6.56 GHz, and at the lower band it covers WiMax (2.5–2.7 GHz). The proposed antenna offers a gain up to 4 dBi with an efficiency up to 90%. The designed antenna is experimented with a partial ground plane, with and without notch to perceive its effects on S_{11} parameters. The antenna and its feed location is optimized for improved performance. The proposed antenna is analysed using the theory of characteristics mode analysis. The antenna is fabricated on a low-cost FR4 substrate with a dielectric constant of 4.4 and a substrate height of 1.6 mm. The antenna performance in terms of S_{11}, VSWR, and Gain is validated by measuring the performance in an anechoic chamber with Agilent N5247A Vector Network Analyser (VNA). The antenna is designed and optimized in mentor graphics software and CST Studio. The results show good agreement between the simulated and measured performances of the antenna. The optimized geometry of the antenna is compact having overall dimensions of 32 mm × 22 mm × 1.6 mm and suitable for short-range IoT applications.

1. INTRODUCTION

With the upsurge in the number of linked devices, the Internet of Things (IoT) has attracted many researchers to face the challenges such as miniaturization of devices, data transmission rate, and data security. Because antenna is an essential component of any communication device, miniaturization of an antenna and its performance improvement have become a major consideration in the research. Lately Telecom Regulatory Authority of India has released a document for providing Narrowband Internet of Things (NBIoT) services with the help of satellite in the areas where no internet services are available [1]. According to CISCO nearly 50 billion devices will be connected using the IoT till the year 2020, which shows a huge scope for connecting tiny sensors [2]. The design of compact antennas for connected devices through IoT enforces a new challenge. RF energy harvesting for powering such sensors is a growing field of interest nowadays [3, 4]. Various techniques have been utilised in the recent literatures to arrive at the desired antenna performance. A slotted antenna directly influences the modal currents and helps in shifting the frequency bands to the desired frequency by choosing the appropriate length and width of slots [5]. The increase in the substrate height and the use of a substrate with reduced dielectric constant help in improving the bandwidth of the antenna, at the cost of increased size and cost, respectively. Compact and multiband antenna for IoT application using the system by design approach enables the fast design of an antenna [6]. Compact and multiband antennas are high in demand for IoT applications. Multiple stubs in the ground plane to give the multiband performance

Received 21 January 2022, Accepted 17 March 2022, Scheduled 30 March 2022
* Corresponding author: Geeta Kalkhambkar (geetakalkhambkar@gmail.com).
[1] Department of ETC, Sant Gajanan Maharaj College of Engineering, Mahagaon, India. [2] Department of ECE, KLE Dr. M. S. Sheshgiri College of Engineering & Technology, Belgaum, India. [3] Department of EE, Sant Gajanan Maharaj College of Engineering, Mahagaon, India.

without altering the radiating patch are discussed in [7]. A hybrid fractal antenna is designed by combining the structural features of Giuseppe Piano, Cantor Set, and Sierpinski Carpet and discussed in [8]. The insertion of a notch at the partial ground plane enhances the antenna performance in terms of gain [8]. The inverse relationship between the lower IoT frequencies and the size of antenna makes it difficult to achieve miniaturization, which is one of the challenges in IoT antenna design. Fractal antenna having self-similarity properties and scaling of initiator to arrive at more compact and optimized structure allows creating more compact antennas. It covers the lower bands of IoT. One such very compact Hilbert curve fractal antenna covering the lower frequencies is discussed in [9]. A cantor set slot embedded in the conventional patch also gives broadband characteristics [10]. Antennas with partial ground plane helps in achieving wideband performance. The use of partial ground plane has become an ideal choice in achieving wideband performance [11]. Coplanar Waveguide (CPW) feed is also found to be the best choice for high bandwidth antennas. Metamaterial antennas are gaining greater importance because of its structure dependent performance and properties to exhibit negative permittivity and permeability. Metamaterials facilitate the improved performance with smaller antenna structures [12]. Fractals are nature-inspired structures, having scaled versions of self-similar shapes repeating at every iteration. Space-filling property fractals provide a choice to miniaturize the antenna structure, yet giving possible resonances at the multiple bands of IoT. Fractals have the inherent ability to achieve multi-band performance as well as broadband performance which depends on the type of fractal shape chosen [13, 14]. Hybrid fractals consisting of a fusion of different fractal shapes together to achieve a unique performance. Hybrid fractals have become a choice for various researchers to innovate the fractal's new capabilities. Various fractal shape antennas are discussed in [15]. Fractal antennas are useful in achieving multifrequency operations [16]. The word fractal was first introduced by B. Mandelbrot [17]. The term fractal is obtained from the word fructus which means broken [18]. T-shaped tuning stub to achieve the notch band characteristics in a cantor-based fractal antenna is discussed in [19]. A similar concept of T-shaped stub is used in [20] to achieve the notch band characteristics in a cantor-shaped fractal antenna, but the insertion of triangular slots and triangular tapered corners in the geometry is used to enhance the bandwidth. Optimization of the feed position is an important parameter in any antenna design process. Curve fitting approach and firefly algorithm gives a direct mathematical relationship between the feed location and resonant frequency which is demonstrated in [21].

In this work a compact cantor set fractal antenna having dual band performance is presented. The antenna serves various IoT applications. The paper is divided into five sections: Section 1 explains the process of designing the cantor set fractal antenna. Section 2 highlights the parametric study. Section 3 describes the modal analysis, and Section 4 shows the results obtained by the simulation and measurement of fabricated antenna. Section 5 provides conclusion with the outcome of the proposed work.

2. ANTENNA DESIGN

The conventional rectangular microstrip antenna is designed to resonate between 2.4 GHz and 2.7 GHz by taking into consideration the empirical equations given in [8]. The cantor-based fractal segments are then constructed iteratively as shown in Figure 1. A rectangular microstrip antenna is taken as an initiator, and fractal slots are created by removing the middle portion in the successive iterations. Fractal dimension D is a non-integer fractional number. The fractal dimension is calculated based on

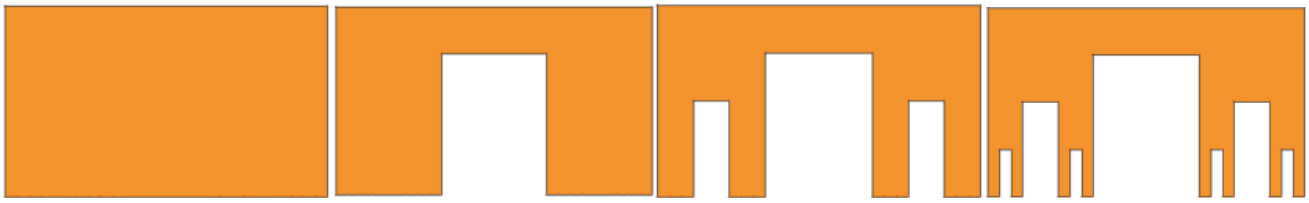

Figure 1. Iterative development of cantor shape fractal antenna.

the expression given in Eq. (1), where ε is the scaling factor, and N is the number of parts of the object. For the proposed geometry, $\varepsilon = 3$ and $N = 2$ are considered.

$$D = \left(\frac{\ln\left(N\left(\varepsilon\right)\right)}{\ln\left(\frac{1}{\varepsilon}\right)} \right) \tag{1}$$

The proposed cantor based fractal geometry is defined by Iterated Function System (IFS) with self-affine transformation as shown in Equation (2).

$$w_i \begin{bmatrix} x \\ y \end{bmatrix} = \begin{bmatrix} a_i & b_i \\ c_i & d_i \end{bmatrix} \times \begin{bmatrix} x \\ y \end{bmatrix} + \begin{bmatrix} e_i \\ f_i \end{bmatrix} \tag{2}$$

The coefficients of IFS are shown in Table 1. Constants in Table 1 lead to the uniform growth of fractal extensions. The variation in these coefficients gives rise to the more complex combination of fractal limbs in the cantor geometry leading to the multi-band performance [22]. In the proposed design, the dimensions of conventional cantor set fractal limbs are unaltered. The geometry is optimized in further iterations based on the density of current distribution responsible for the performance in the particular frequency of interest. Cantor set-based fractal geometries have an inherent capability to offer a wideband performance and dual-band S_{11} characteristics [10, 15, 16, 19]. The dual-band performances offered by previous experimental works on cantor set fractal geometry are based on the original dimension of the initiator chosen for the geometry construction. The middle portion which is removed causes the cantor set antenna to behave as two separate antennas, one resonating at the lower band and the second portion resonating at the higher band. The optimization of the geometry based on current distribution helps in identifying the optimum feed location. It is expressed in the final optimized geometry of the proposed design as shown in Figure 3.

Table 1. Coefficients of IFS.

w_i	a_i	b_i	c_i	d_i	e_i	f_i
1	0.3	0	0	1	0	0
2	0.3	0	0	1	0.6	0

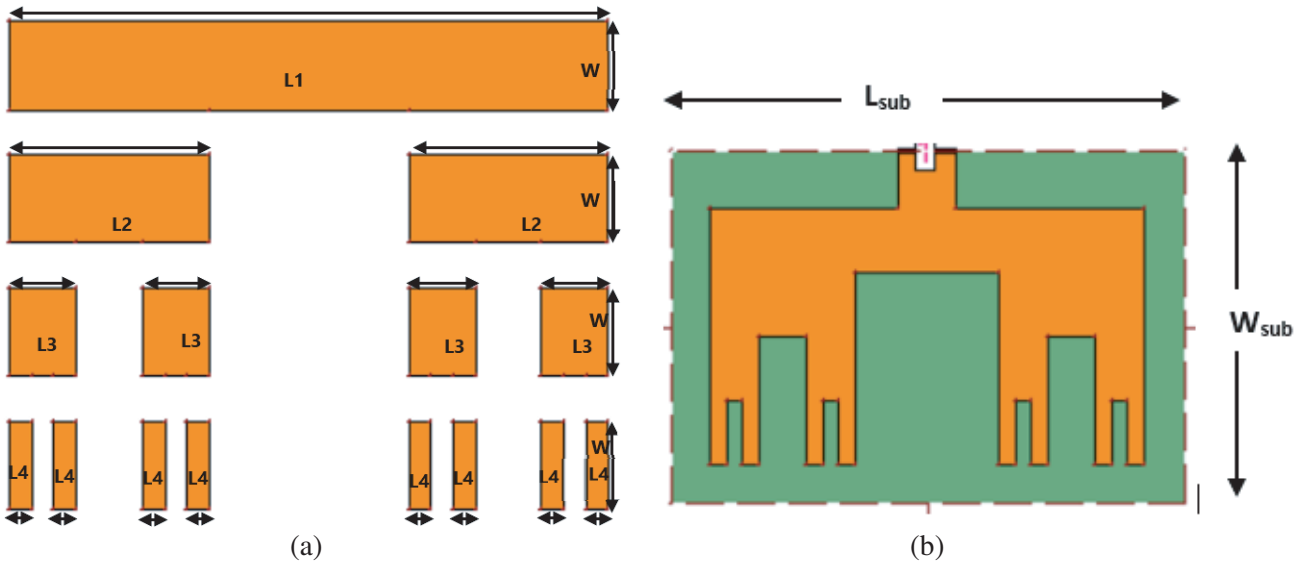

Figure 2. Pictorial representation of the detailed dimensions of the proposed antenna. (a) Fractal dimensions. (b) Substrate dimensions.

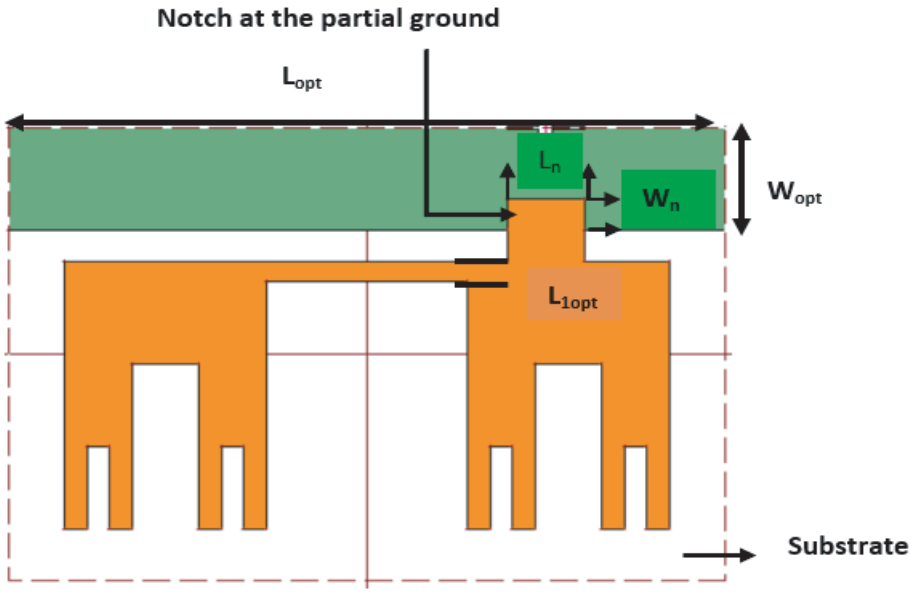

Figure 3. Optimized geometry.

The geometry is designed on an FR4 substrate with dielectric constant 4.4 and substrate height 1.6 mm with overall dimensions of the substrate 32 mm × 22 mm × 1.6 mm. The detailed dimensions of the geometry are given in Table 2 and are designated in Figure 2(a) and Figure 2(b). The geometry is optimized for a partial ground plane, and the notch is inserted at the ground plane to arrive at the optimum output as depicted in Figure 3. Figure 3 shows the geometry after optimization. The partial ground plane reduces the surface wave diffraction from the corners and helps to enhance the front to back ratio of the antenna and hence improves the antenna performance [23]. The antenna is simulated with a line feed, and the line feed location is also optimized for the desired outcome. Table 2 includes the optimized geometry dimensions.

Table 2. Dimensions of the proposed antenna.

Parameters	Dimensions in mm
W	4
L1	27
L2	$L2 = L1/3 = 9$
L3	$L3 = L1/9 = 3$
L4	$L4 = L1/27 = 1$
$\mathbf{L_{sub}}$	32
$\mathbf{W_{sub}}$	22
$\mathbf{W_{opt}}$	5
$\mathbf{L_{opt}}$	32
$\mathbf{L_{1opt}}$	01
$\mathbf{L_n}$	3.5
$\mathbf{W_n}$	1

3. PARAMETRIC STUDY

Figure 4 represents the improvement in S_{11} characteristics from an initiator to the final optimized geometry of the proposed antenna. The final iteration gives better results than the initial iterations. The geometry is modified for the partial ground and the notch at the partial ground with the optimized dimension of portion L1 evident in Figure 2 and Figure 3. Portion L1 is the deciding factor for controlling the resonant frequency and bandwidth because of the factor that the current distribution is more prominent along L1. On reducing the width of L1 the current along the X direction is influenced as indicated in Figures 12(a)–(c), and the modal current TM_{100} is enhanced causing the antenna to behave like two different antennas resonating at two isolated bands. By locating the feed position near the rightmost portion of antenna, the second band current is more pronounced giving the wideband performance in the second band due to the excitation of higher order modes. Figure 12 shows the surface current distribution at 2.4 GHz, 5 GHz, and 8.5 GHz simulated using mentor graphics tool.

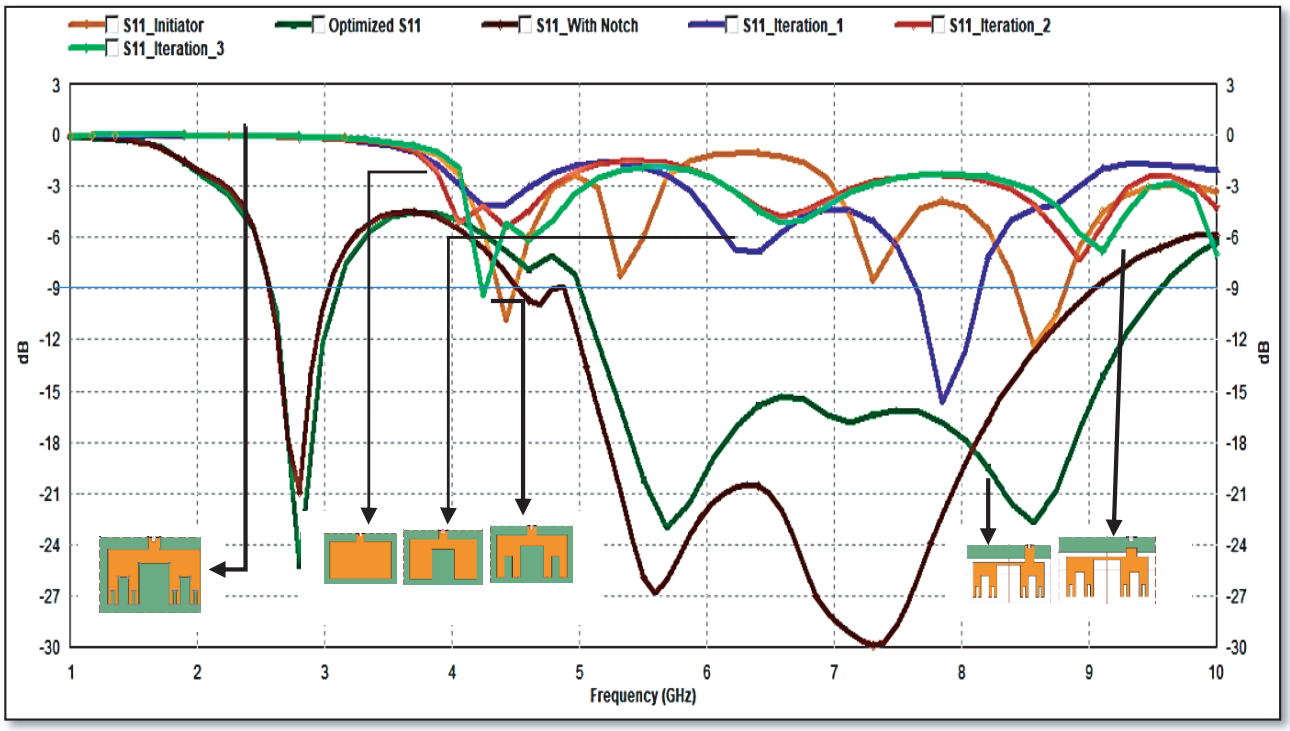

Figure 4. Parametric study on iterative progression and refinement of the proposed antenna.

4. MODAL ANALYSIS

Characteristics Mode Analysis (CMA) is an efficient tool to forecast the natural resonance for material without any feed information. The governing equations of CMA derived from the impedance metrics are described in Equations (3)–(6).

$$Z = R + jX \tag{3}$$

$$XJ_n = \lambda_n RJ_n \tag{4}$$

R indicates the Hermitian Real part of Z matrix; X indicates the Hermitian Imaginary part of Z matrix; Jn indicates the eigen current; λn depicts the eigenvalue.

Eigenvalue, Modal significance, and the characteristics angle are the important parameters to observe in case of CMA. Modal significance shows the contribution of particular mode in the radiation

and is given by Equation (3), and its range is 0 to 1.

$$MS = \left| \frac{1}{1+j\lambda_n} \right| \tag{5}$$

Characteristic angle signifies the resonant frequency of a mode at resonance, $\lambda_n = 0$ and $\alpha_n = 180°$

$$\alpha_n = 180° - \tan^{-1}(J_n) \tag{6}$$

Eigenvalue at resonance is zero, which means that modes are radiating, when $\lambda_n < 0$ modes are storing electric energy. $\lambda_n > 0$ indicates that modes are storing magnetic energy. For an efficient radiator, the ideal value for λ_n is 0.

The modal analysis is carried out in CST Microwave studio. An eigenvalue, modal significance, and the characteristics angle are observed for the first five resonant modes. It is observed that the

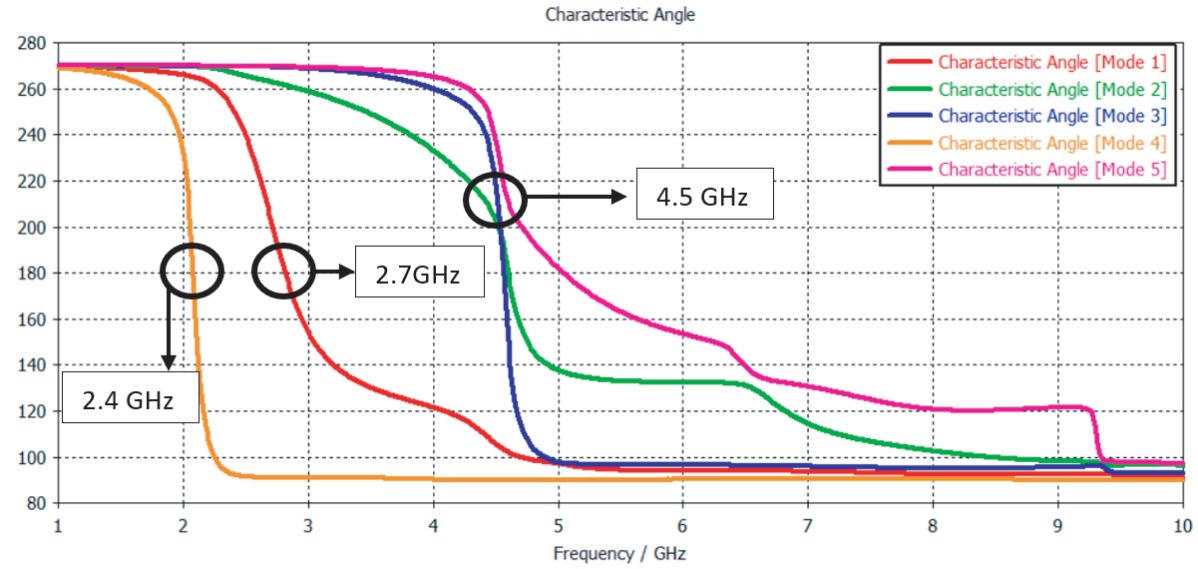

Figure 5. Characteristics angle plot.

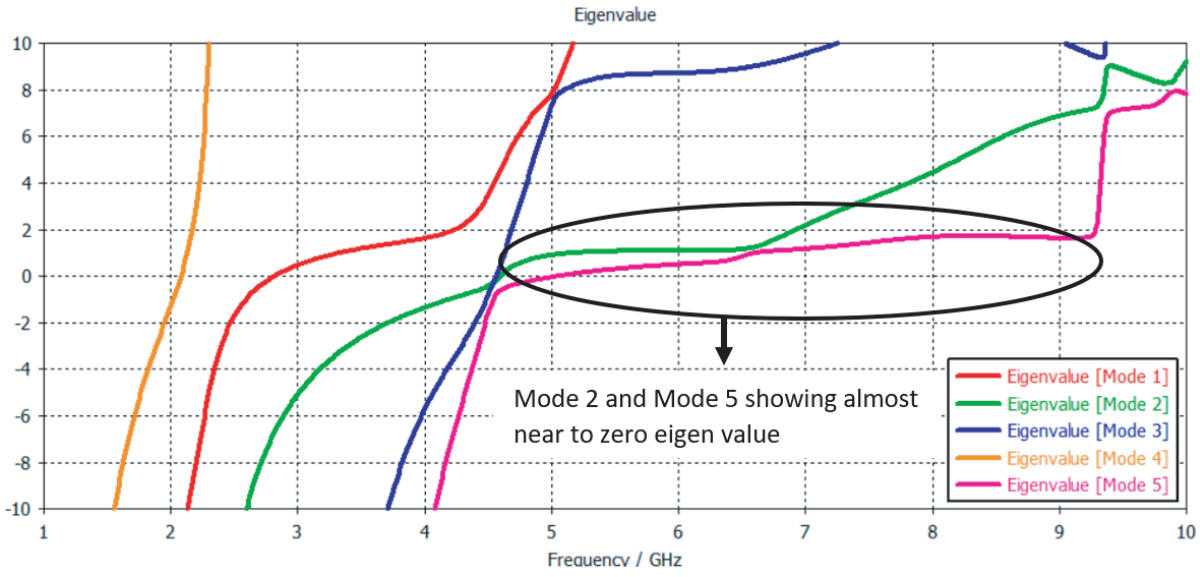

Figure 6. Eigenvalue plot.

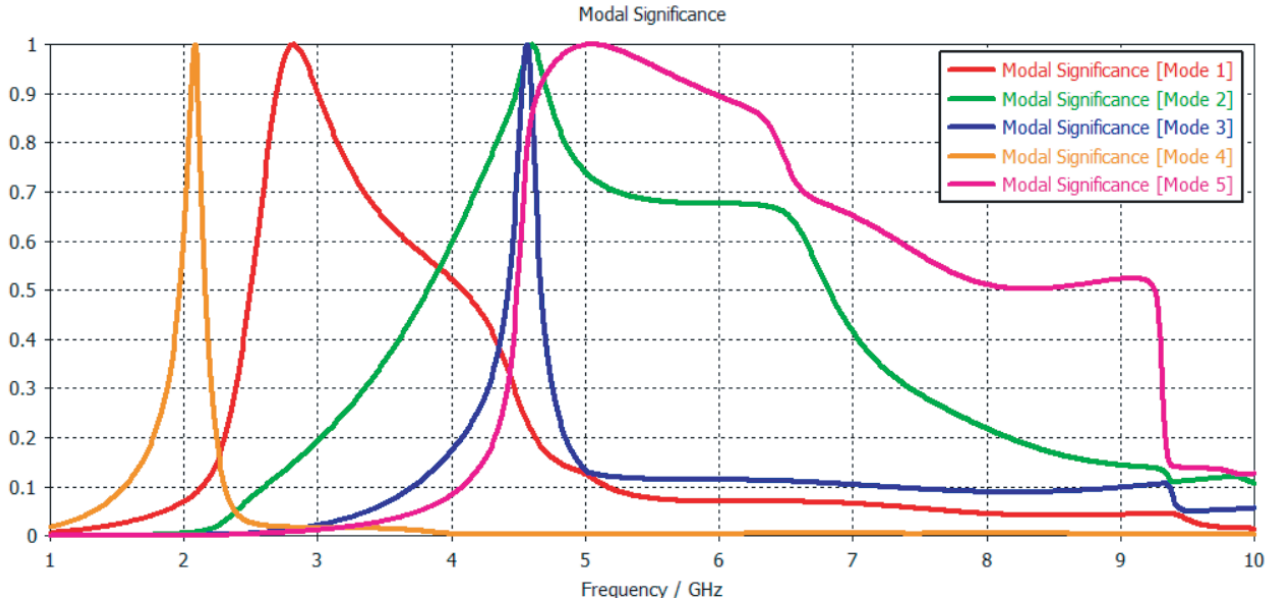

Figure 7. Modal Significance plot.

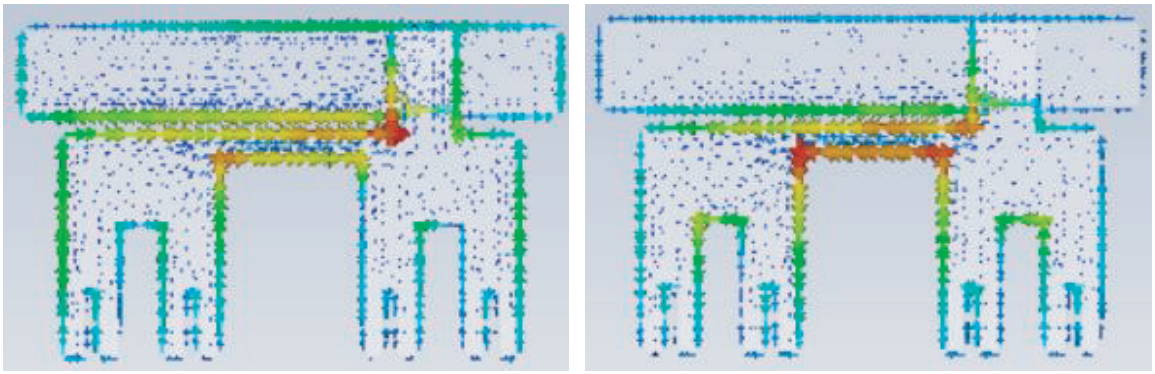

Figure 8. Modal currents Mode 1 & Mode 4 Resonating at 2.4 GHz.

band at 2.4 GHz is influenced by mode 1 and mode 4 crossing 180° line in characteristics angle plot in the range 2.4 GHz to 2.7 GHz. The second band is a result of exciting mode 2, mode 3, and mode 5 crossing 180° at 4.5 GHz as shown in Figure 5. Mode 2 and mode 5 show almost stable eigenvalue at the second band starting from 4.5 GHz to nearly 9 GHz giving the wideband behavior as shown in Figure 6. The modal significance at the desired bands is observed as shown in Figure 7. The value of modal significance is observed to be 1 at the desired bands 2.4 GHz and 5 GHz. Beyond 5 GHz, a gradual decrease in the modal significance at mode 2 and mode 5 is observed. At higher frequencies, stable current distribution produces wideband behavior from 5 GHz to 8.5 GHz since modal significance decreases gradually. Figure 8 and Figure 9 depict the modal currents simulated using characteristics mode analysis. The feed location can be experimented to excite the modes of interest, and hence the desired resonance and bandwidth are achievable in the further study.

5. RESULTS AND ANALYSIS

The proposed antenna with and without notch is simulated using mentor graphics software. The improvement in S_{11} parameter is observed after the insertion of a notch in the ground plane. This effect is due to the enhanced current distribution on the surface of the monopole and the ground plane

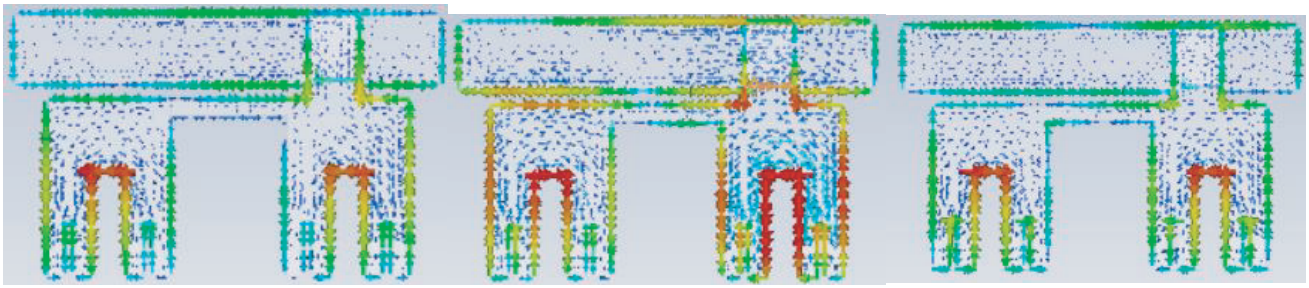

Figure 9. Modal currents Mode 2, Mode 3 & Mode 5 Resonating at 5 GHz to 8.5 GHz.

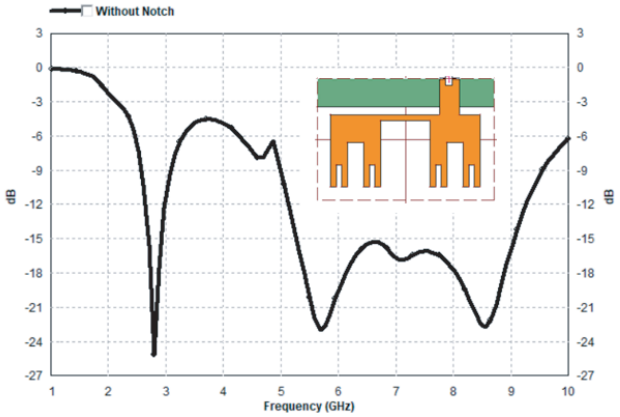

Figure 10. S_{11} before the insertion of notch.

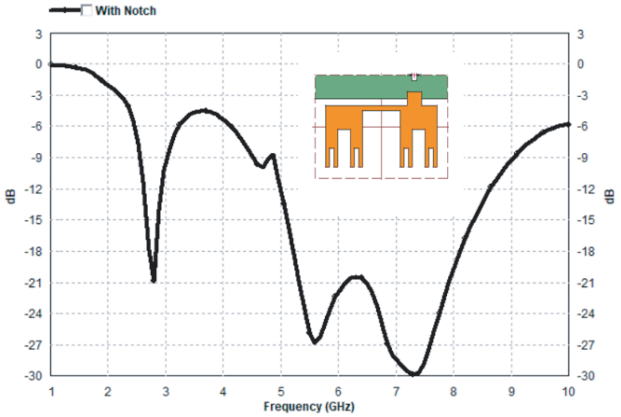

Figure 11. S_{11} after the insertion of notch.

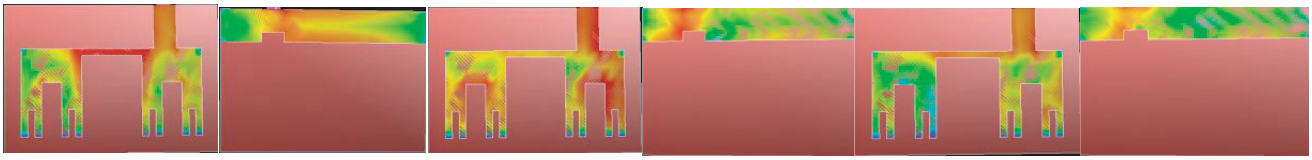

(a) (b) (c)

Figure 12. Current distribution. (a) At 2.4 GHz. (b) At 5 GHz. (c) At 8.5 GHz

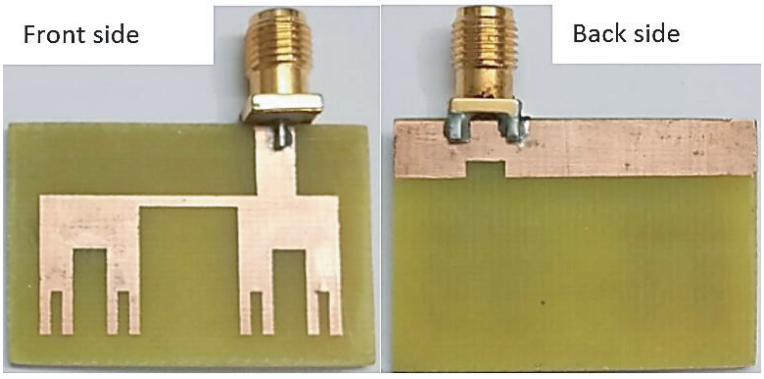

Figure 13. Fabricated images.

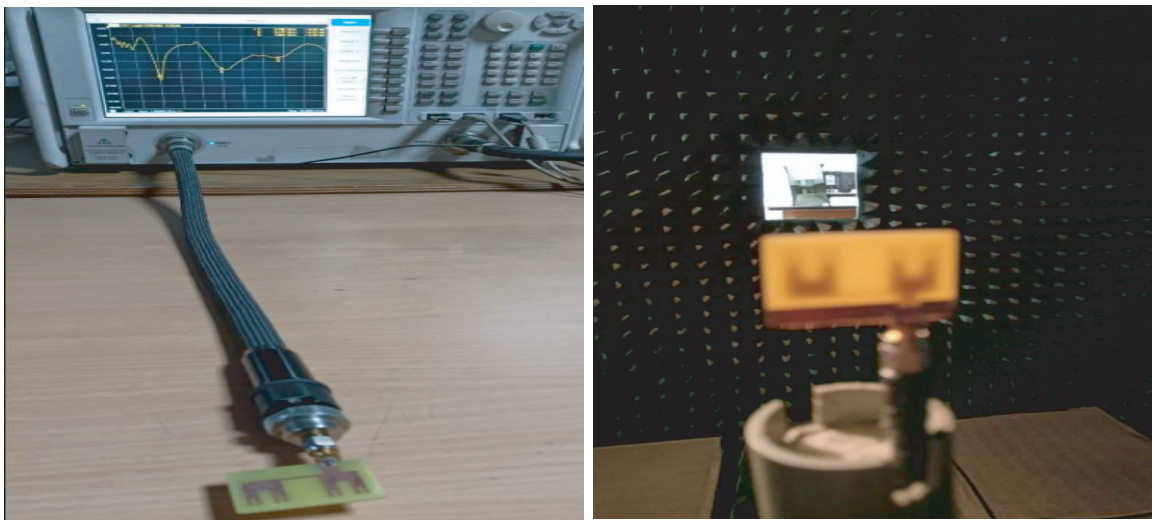

(a) (b)

Figure 14. (a) Proposed antenna connected to VNA. (b) Proposed antenna connected in an Anechoic Chamber.

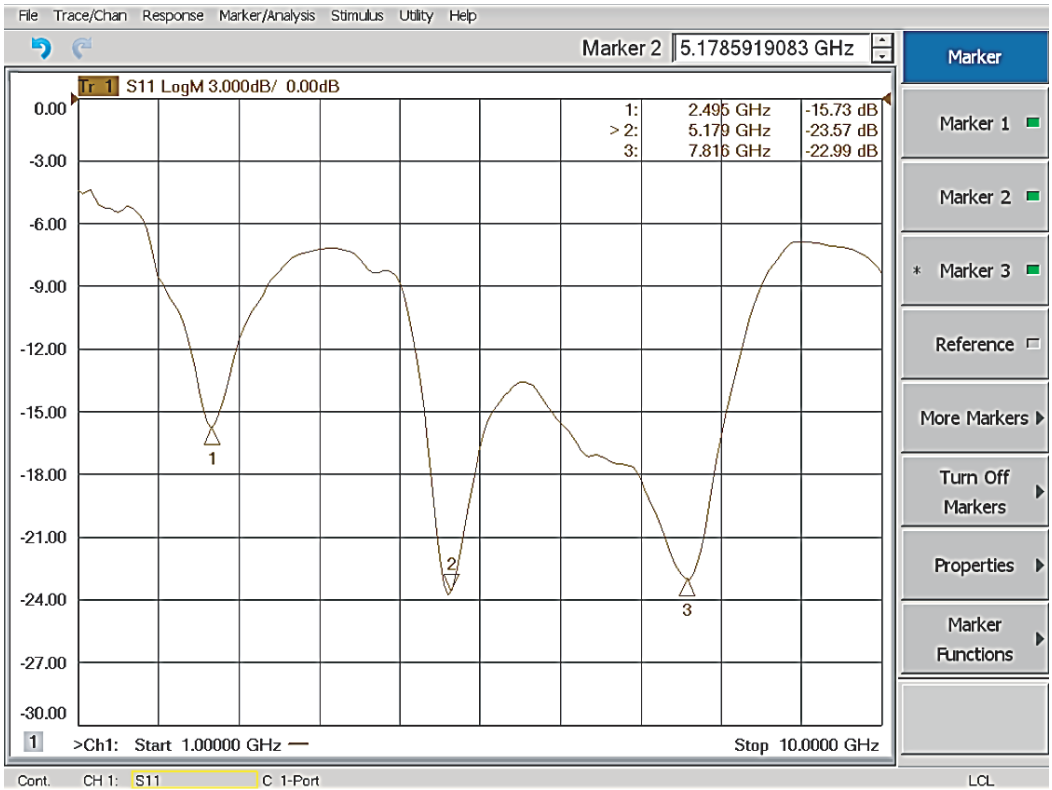

Figure 15. Measures S_{11} on VNA.

as shown in Figure 12. The optimized portion of L1 (L1opt) contributes more at the lower frequency whereas L2, L3, and L4 contribute at the higher frequency. The notch in the partial ground causes the increase in the electrical length of the ground plane and hence helps in matching the impedance. The VSWR plot depicted in Figure 19 shows the impact of notch on matching the antenna input impedance

to the 50 Ω port. This results in improved S_{11} characteristics as depicted in Figure 10 and Figure 11.

The geometry is simulated in CST Microwave studio to ensure the accuracy of the design simulated in mentor graphics, and the CST simulated S_{11} and the mentor graphics simulated S_{11} show nearly matching resonances. The proposed antenna is fabricated on an FR4 substrate, and the measurements are carried out in an anechoic chamber. Figure 13 shows the geometry of fabricated antenna, and

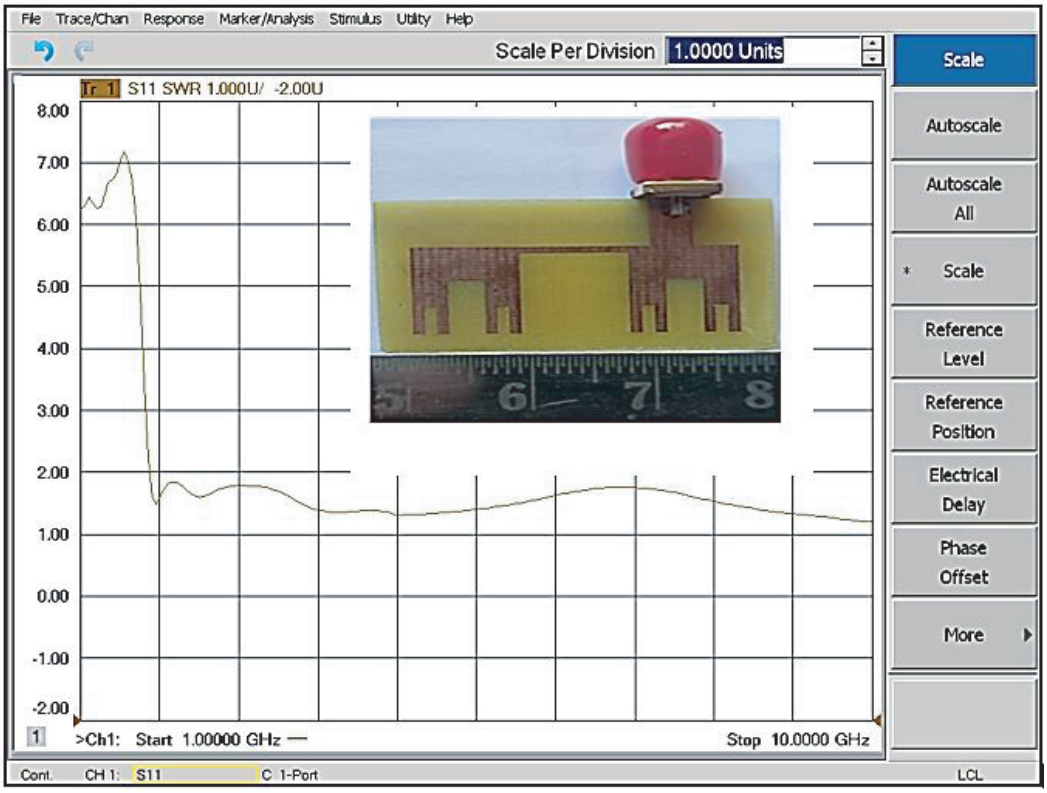

Figure 16. Measures VSWR on VNA.

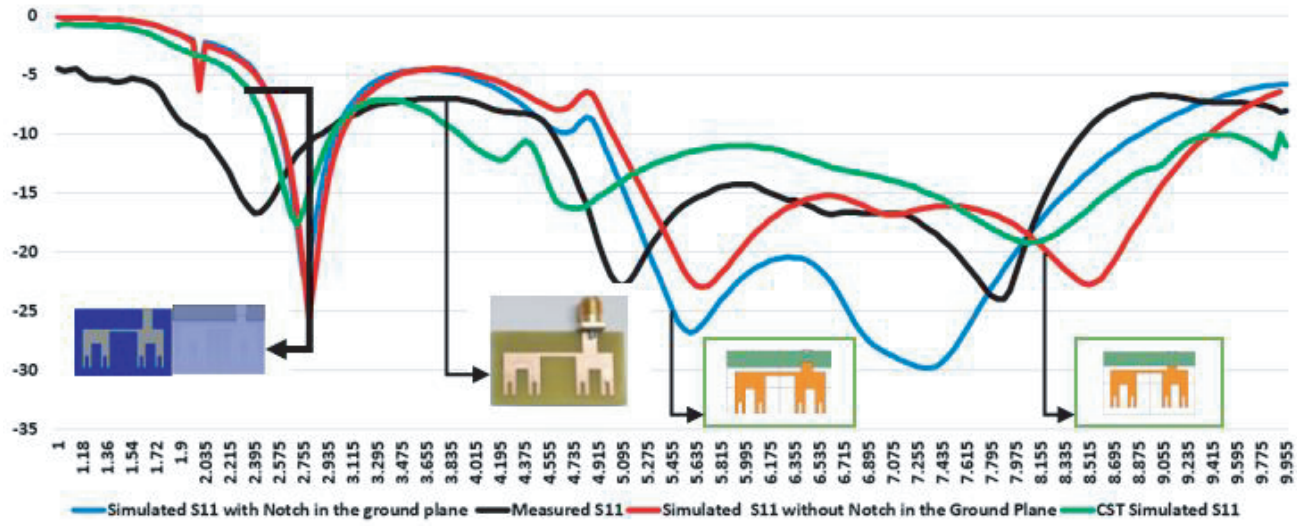

Figure 17. S_{11} comparison of Mentor graphics simulation, CST simulation and Measured results.

Figure 14(a) shows the antenna connected to VNA with measured S_{11} parameters displayed on it, also shown in Figure 15. Figure 16 shows the measured VSWR plot. Figure 14(b) indicates the antenna measurement carried out in an anechoic chamber. The S_{11}, VSWR, and gain of the antenna are measured. Figure 17 shows the comparison of S_{11} simulated in Mentor Graphics and CST Microwave studio, with the measured S_{11} from a vector network analyser. Figure 19 shows the comparison between VSWR of geometry with a notch and that without a notch in the ground plane. It shows that the insertion of notch gives improved VSWR because of improvement in the impedance matching. The results from Mentor Graphics CST and measured results from VNA are in close agreement and within the accepted range with less than 10% deviation in the results.

The peak gain up to 3.6 dBi is achieved, and the gain is measured in an anechoic chamber using

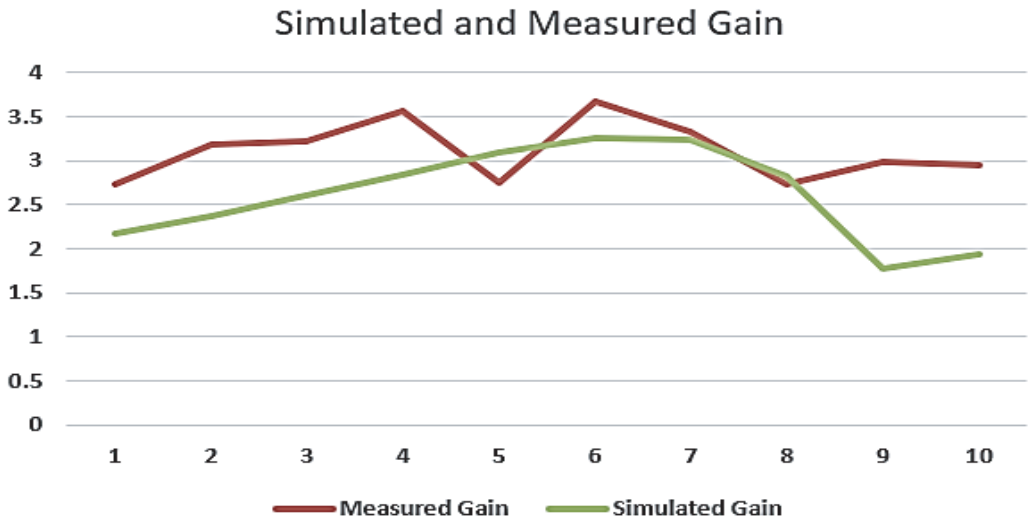

Figure 18. Simulated and measured gain.

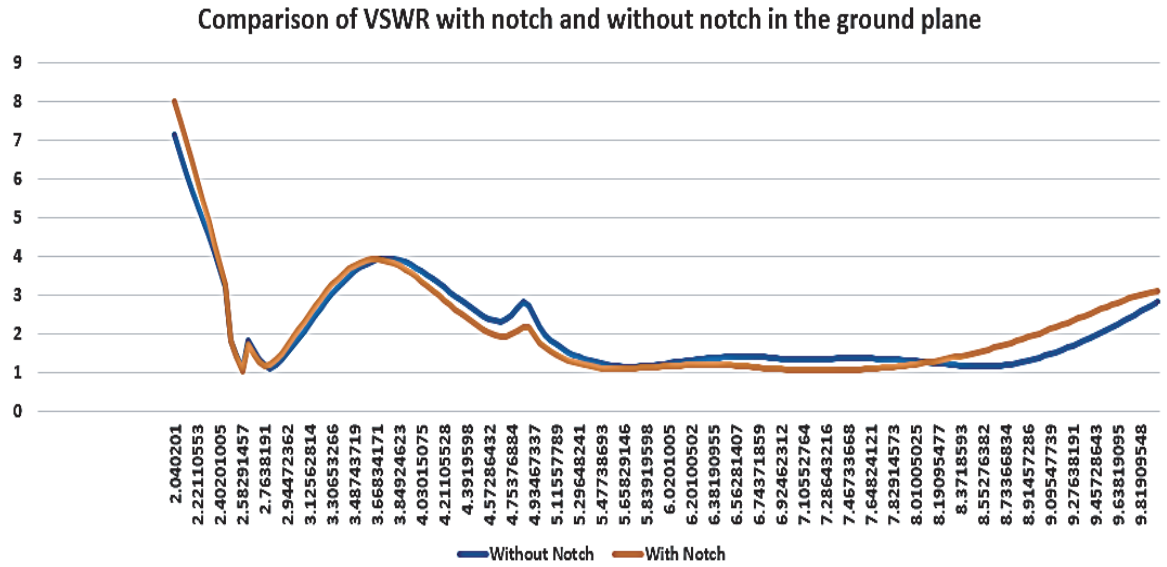

Figure 19. VSWR with and without notch.

Equation (7)

$$G_{AUT} = \left(\frac{P_{R2}}{P_{R3}}\right) * G_{REF} \tag{7}$$

where P_{R2} = *Received power by reference antenna*, P_{R3} = *Received power by antenna under test*, G_{REF} = *Gain of reference antenna*.

Figure 18 shows the comparison between the software simulated gain and measured gain. The minor

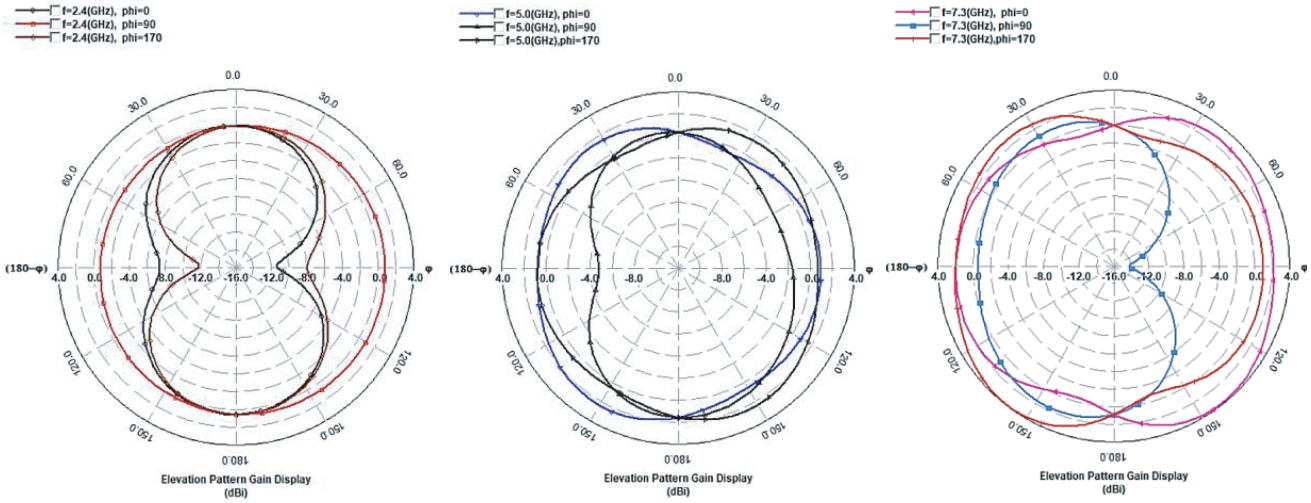

(a) (b) (c)

Figure 20. (a) Radiation pattern at 2.4 GHz. (b) Radiation pattern at 5 GHz. (c) Radiation pattern at 7.5 GHz.

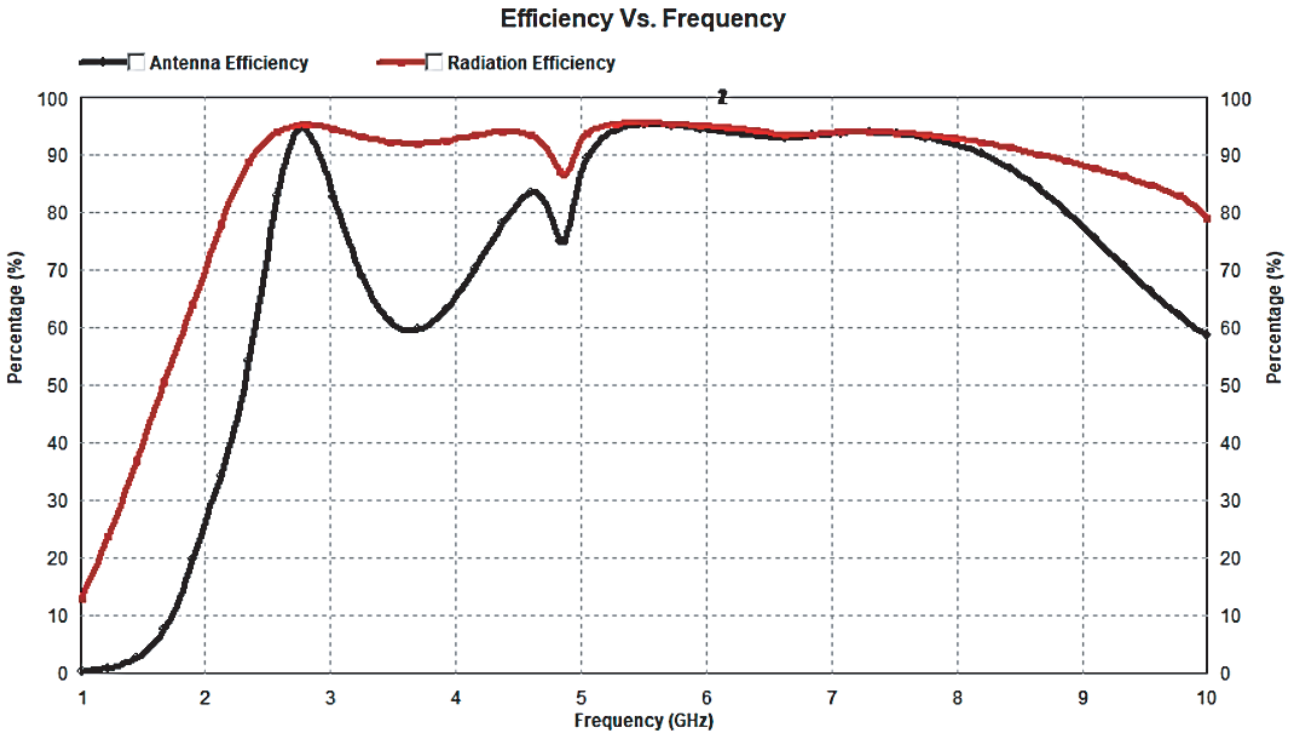

Figure 21. Antenna efficiency and Radiation efficiency.

disagreement in the results is due to the fringing field created because of asymmetric feed placement and fabrication imperfections.

Figure 20 shows the simulated radiation patterns at 2.4 GHz, 5 GHz, and 7.5 GHz, respectively. Elevation pattern gain display at 2.4 GHz is bidirectional at phi = 0 and phi = 90 degrees and omnidirectional at phi = 170 degrees. The radiation patterns at 5 GHz and 7.5 GHz are almost omnidirectional. The proposed antenna radiates with an efficiency of near 90% at the desired bands as shown in Figure 21. The proposed antenna is compared with the recently published research work in Table 3. The proposed antenna shows better performance in terms of size and bandwidth than the recent literature, making it suitable for IoT applications. Antenna proposed in [9] is more compact in size, but the proposed antenna outperforms it in terms of bandwidth and gain which are equally important in IoT applications for improved data transmission rate.

Table 3. Comparison of proposed antenna with recent literatures.

Ref.	**Antenna Type**	**Substrate**	**Resonant frequencies in GHz**	**Dimension's in mm**	**Peak gain in dBi**	**Bandwidth**
[5]	Square slotted	Rogers RT5880	2.4, 2.8	38.5 × 38.5	3.45, 3.2	20 MHz, 220 MHz
[7]	multiple resonant stubs	FR4	2.45/5.2/5.8 2.8/3.8/5.5	43 × 33	5.5, 4.4, 0.0 2.45, 2.8, 3.8,	2.28–3.10 GHz (30.4%), 3.52–4.10 GHz (15.2%), and 5.05–6.00 GHz (17.2%).
[8]	Hybrid fractal	FR4	2.4411, 5.7389, 2.4341	34 × 34	8.39, 7.17, 14.84	101 MHz
[9]	Hilbert curve Fractal	FR-4	1.8 3.3 5.5	18 × 16.5	0.27, 1.33 and 2.27	150, 390, 2610 (MHz range)
[10]	Cantor set fractal slots	FR4	3.7/5.9	31 × 28	3.2; 4.15	3.3, 3.3 (GHz range)
[11]	Nested square shaped ring fractal	FR4	2.4/4.8/7.8 /11.7/16.5	36 × 32	Not Mentioned	3.23 GHz
[19]	Cantor set based hybrid fractal	FR4	2.4400 and 5.8115	34 × 34	10.19, 5.74	Not Mentioned
Proposed Antenna	**Cantor set fractal**	**FR4**	**2.4–2.7, 5.0 to 8.5**	**32 × 22**	**2.0, 3.8**	**First band: 420 MHz Second band: 4 GHz**

6. CONCLUSION

A four-level iterated cantor-based fractal antenna is designed, optimized, and observed in terms of its performance. the cantor-based fractal antenna with partial ground results in a wideband performance. Insertion of a notch at the partial ground improved the S_{11} characteristics. The characteristics mode analysis helps in forecasting the antenna performance and also helps in choosing the appropriate feed location for the desired performance. The proposed antenna after optimization covers 2.4 GHz to 2.7 GHz and 5 GHz to 8.5 GHz frequencies. The proposed antenna is suitable for the Wi-Fi 802.11 standard applications (2.4 GHz, 4.9 GHz, 5 GHz, 5.9 GHz, 6 GHz), WiMax (2.5–2.7 GHz) and 6.56 GHz band, ITU band (7.8–8.4 GHz), television broadcasting (7.91–8.62 GHz), point-to-point wireless applications (5.92–8.5 GHz), and WLAN (2.4–2.48 GHz, 5.15–5.35 GHz). The proposed antenna having small size and light weight serves as a good candidate for the IoT applications.

REFERENCES

1. "Consultation Paper on Licensing Framework for Satellite-based connectivity for low bit rate applications," Telecom Regulatory Authority of India, March 12, 2021.
2. Gupta, A. K., P. S. R. Chowdary, and M. Vamshi Krishna, "Trends in IoT antenna design — A brief review," *Test Engineering and Management*, 14198–14203, July 2020, ISSN: 0193-4120.
3. Chindhi, P. S., H. P. Rajani, G. B. Kalkhambkar, and R. Khanai, "Characteristics mode analysis of modified inset-fed microstrip antenna for radio frequency energy harvesting, biosc," *Biotech. Res. Comm.*, Special Issue, Vol. 13, No. 13, 171–176, 2020.
4. Chindhi, P. S., H. P. Rajani, and G. B. Kalkhambkar, "A tapered slot rectangular ultra-wideband microstrip patch antenna for radio frequency energy harvesting," *Futuristic Communication and Network Technologies*, 373–383, 2019.
5. Abdulkawi, W. M., A. F. A. Sheta, I. Elshafiey, and M. A. Alkanhal, "Design of low-profile single- and dual-band antennas for IoT applications," *Electronics*, Vol. 10, 2766, 2021.
6. Salucci, M., N. Anselmi, S. Goudos, and A. Massa, "Fast design of multiband fractal antennas through a system-by-design approach for NB-IoT applications," *EURASIP Journal on Wireless Communications and Networking*, Vol. 2019, 68, 2019.
7. Jing, J., J. Pang, H. Lin, Z. Qiu, and C. Liu, "A multiband compact low-profile planar antenna based on multiple resonant stubs," *Progress In Electromagnetics Research Letters*, Vol. 94, 1–7, 2020.
8. Kaur, M. and J. S. Sivia, "ANN and FA based design of hybrid fractal antenna for ISM band applications," *Progress In Electromagnetics Research C*, Vol. 98, 127–140, 2020.
9. Samson Daniel, R., "Asymmetric coplanar strip-fed with Hilbert curve fractal antenna for multiband operations," *Wireless Personal Communications*, Vol. 116, No. 1, 791–803, 2020.
10. Ez-Zaki, F., H. Belahrach, and A. Ghammaz, "Broadband microstrip antennas with Cantor set fractal slots for vehicular communications," *International Journal of Microwave and Wireless Technologies*, 1–14, 2020.
11. Bharti, G. and J. S. Sivia, "A design of multiband nested square shaped ring fractal antenna with circular ring elements for wireless applications," *Progress In Electromagnetics Research C*, Vol. 108, 115–125, 2021.
12. Chindhi, P. S., G. B. Kalkhambkar, H. P. Rajani, and R. Khanai, "A brief survey on metamaterial antennas: Its importance and challenges," *Futuristic Communication and Network Technologies*, 425–432, 2020.
13. Kalkhambkar, G., R. Khanai, and P. Chindhi, "Fractals: A novel method in the miniaturization of a patch antenna with bandwidth improvement, information and communication technology for intelligent systems," *Smart Innovation, Systems and Technologies*, 106, 2019.

14. Kalkhambkar, G., R. Khanai, and P. Chindhi, "Design and analysis of wideband polygonal microstrip fractal patch antenna with three dimensional finite difference time domain method and UPML boundaries," *International Journal of Advanced Research in Engineering and Technology (IJARET)*, Vol. 11, No. 9, 323–336, Article ID: IJARET_11_09_033, September 2020.
15. Sharma, N. and S. S. Bhatia, "Comparative analysis of hybrid fractal antennas: A review," *Int. J. RF Microw. Comput. Aided Eng.*, e22762, 2021.
16. Anguera, J., C. Puente, C. Borja, and J. Soler, "Fractal shaped antennas: A review," *Encyclopedia of RF and Microwave Engineering*, https://doi.org/10.1002/0471654507.eme128, 2005.
17. Mandelbrot, B. B., *The Fractal Geometry of Nature*, ISBN 0-7167-1186-9, w. 320 H. Freeman and Company, New York, 1983.
18. Anguera, J., A. Andújar, J. Jayasinghe, V. V. S. S. Sameer Chakravarthy, P. S. R. Chowdary, J. L. Pijoan, and T. A. C. Cattani, "Fractal antennas: An historical perspective, MDPI," *Fractal Fract.*, Vol. 4, No. 1, 3, 2020.
19. Li, Y. S., X. D. Yang, C. Y. Liu, and T. Jiang, "Analysis and investigation of a cantor set fractal UWB antenna with a notch-band characteristic," *Progress In Electromagnetics Research B*, Vol. 33, 99–114, 2011.
20. Terlapu, S. K., P. S. R. Chowdary, C. Jaya, V. V. S. S. Sameer Chakravarthy, and S. C. Satpathy, "On the design of fractal UWB wide-slot antenna with notch band characteristics, microelectronics, electromagnetics and telecommunications," *Lecture Notes in Electrical Engineering*, 471, 2018.
21. Kaur, M. and J. S. Sivia, "Giuseppe Peano and Cantor set fractals based miniaturized hybrid fractal antenna for biomedical applications using artificial neural network and firefly algorithm," *Int. J. RF Microw. Comput. Aided Eng.*, Vol. 2019, e22000, 2019.
22. Manimegalai, B. annd S. Raju, "A multifractal cantor antenna for multiband wireless applications," *IEEE Antennas and Wireless Propagation Letters*, Vol. 8, 2009.
23. Lee, H.-M., "Effect of partial ground plane removal on the front-to-back ratio of a microstrip antenna," *2013 7th European Conference on Antennas and Propagation (EuCAP)*, 2013.